

Synthesis and conformational behavior of the difluoromethylene linked C-glycoside analog of β -galactopyranosyl-(1 \leftrightarrow 1)- α -mannopyranoside

Richard W. Denton,^{a,b} Kurissery A. Tony,^{a,b} José Juan Hernández-Gay,^c
F. Javier Cañada,^c Jesús Jiménez-Barbero^{c,*} and David R. Mootoo^{a,b,*}

^aDepartment of Chemistry, Hunter College, 695 Park Avenue, New York, NY 10021, United States

^bThe Graduate Center, CUNY, 365 5th Avenue, New York, NY 10016, United States

^cCentro de Investigaciones Biológicas, CSIC, Ramiro de Maeztu 9, 28040 Madrid, Spain

Received 14 March 2007; received in revised form 6 June 2007; accepted 7 June 2007

Available online 13 June 2007

Abstract—C-Glycosides in which the pseudoglycosidic substituent is a methylene group have been advertised as hydrolytically stable mimetics of their parent O-glycosides. While this substitution assures greater stability, the lower polarity and increased conformational flexibility in the intersaccharide linker brought about by this change may compromise biological mimicry. In this regard, C-glycosides, in which the pseudoanomeric methylene is replaced with a difluoromethylene group, are interesting because the CF₂ group is more of an isopolar replacement for oxygen than CH₂. In addition, the CF₂ residue is expected to instill conformational bias into the intersaccharide torsions. Herein is described the synthesis and conformational behavior of the difluoromethylene linked C-glycoside of β -D-galactopyranosyl-(1 \leftrightarrow 1)- α -D-mannopyranoside. The synthesis centers on the formation of the galactose residue via an oxocarbenium ion–enol ether cyclization. Conformational analysis, using a combination of molecular mechanics, dynamics, and NMR spectroscopy, suggests that the difluoro-C-glycoside populates the non-*exo*-Gal/*exo*-Man conformer to a major extent (ca 50%), with a minor contribution (~15%) from the *exo*-Gal/*exo*-Man conformer that corresponds to the ground state of the parent O-glycoside.

© 2007 Elsevier Ltd. All rights reserved.

Keywords: Glycomimetic; Oxocarbenium ion; Cyclization; De novo

1. Introduction

The replacement of the glycosidic oxygen in O-glycoside with a methylene substituent leads to an analogue with greater hydrolytic stability than the parent O-glycoside.¹ Such compounds often referred to as exact C-glycosides, may function as biological mimetics of their parent O-glycosides, but the extent of this mimicry could be compromised by the lower polarity and greater flexibility of the intersaccharide linker.^{2–5} In this vein, we have been

interested in the mimicry of C-glycosides in which the methylene linker is replaced with a CHF or CF₂ residue. The design of these mimetics was guided by two tenets. First, the electronegativity of the fluorine substituents could make the intersaccharide linker more isopolar to the glycosidic oxygen.⁶ Second, based on the unusual conformational properties of 2-fluoroethanols and related structures, such fluoro-C-glycosides are expected to have a more well defined conformational bias than the exact C-glycoside with respect to the intersaccharide linker, such that they may more closely mimic the conformational properties of O-glycoside.^{7,8} Indeed, the use of CHF and CF₂ as isosteres of oxygen has been examined in other molecules of biological interest, and examples of CF₂ linked C-furanosides have been

* Corresponding authors. Tel.: +34 918373112x4370; fax: +34 915531706 (J.J.-B.); tel.: +1 212 772 4356; fax: +1 212 772 5332 (D.R.M.); e-mail addresses: jjbarbero@cib.csic.es; d mootoo@hunter.cuny.edu

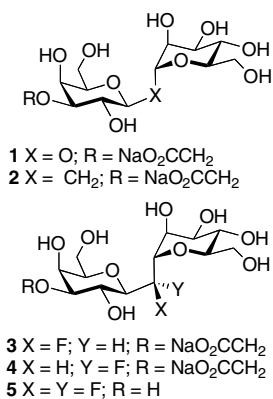


Figure 1. O- and C-disaccharides.

prepared.^{9–11} We have previously reported the synthesis and conformational behavior of **2–4**,^{12,13} the exact and the CHF linked analogues of **1**, a known O-disaccharide mimetic of sialyl Lewis X (Fig. 1).¹⁴ In this series the fluoro-C-glycoside **3** was found to be the closest conformational mimic of **1**. Herein, as an extension of this study, we describe the synthesis and conformational properties of the CF₂ linked analogue **5**.¹⁵

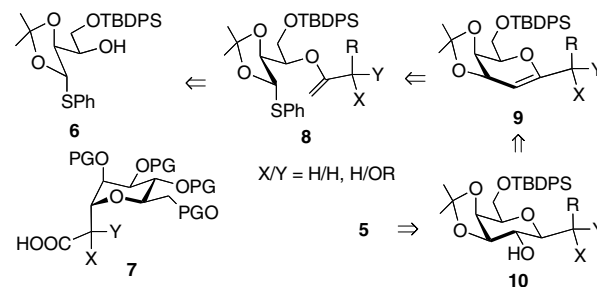
2. Results and discussion

2.1. Synthesis

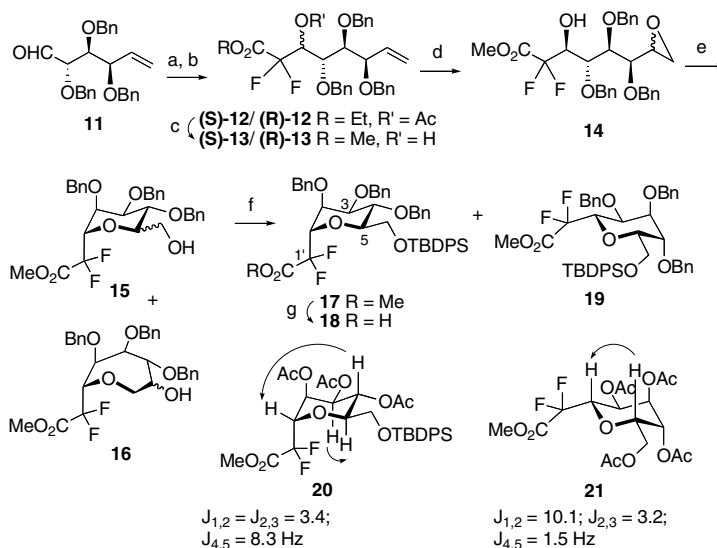
We have been developing a de novo synthesis of complex C-disaccharides **10**, in which the key step is the formation of a C1 substituted glycal **9** via an enol ether–oxocarbenium ion cyclization.¹⁶ C-Glycoside **10** is then obtained by the stereoselective hydroboration of **9**. Because this method was previously successful

for hydroxymethyl linked C-glycosides (e.g., **10**: X/Y = H/OH), we envisaged an initial synthesis of **5** that was based on fluorination of the ketone derived from **10**.¹⁷ Not surprisingly, given the highly substituted nature of this precursor, this strategy was unsuccessful. Therefore, a revised plan in which the CF₂ group was introduced in a less complex precursor (i.e., **7**: X/Y = F/F) was adopted. A key question with this approach was the feasibility of the oxocarbenium ion cyclization on the difluorinated enol ether thioacetal (i.e., **8**, X/Y = F/F) in light of the noted deactivation of related difluorinated enol ethers to electrophilic reagents.¹⁸ In addition, while the thioacetal precursor **5** was available from earlier investigations, a synthesis of an α,α -difluoroacid like **7** had to be devised (Scheme 1).

Initial attempts at the synthesis of α,α -difluoroacid through treatment of an α -ketoester precursor with DAST¹⁷ led to intractable mixture of products. A successful plan originated in the reaction of the Reformatsky-like reagent from methyl bromodifluoroacetate and the known aldehyde **11** (Scheme 2).^{19,20} This led to an inseparable mixture of epimeric (*R*)- and (*S*)-alcohols



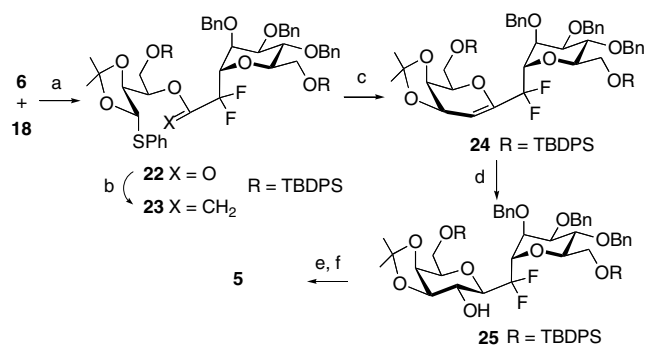
Scheme 1. Retrosynthesis of the difluoromethylene linked C-disaccharide.



Scheme 2. Synthesis of difluoroacid **18**. Reagents: (a) BrCF₂CO₂Et, Zn, THF, reflux then **11**; (b) Ac₂O, DMAP, EtOAc, two steps, 35%; (c) NaOMe, MeOH, 83%; (d) *m*CPBA, CH₂Cl₂, aq NaH₂PO₄/Na₂HPO₄, 74%; (e) (i) NaOMe, MeOH then HCl in ether; (ii) TMSCHN₂, MeOH, **15** (52%) + **16** (22%); (f) TBDPSCl, imidazole, DMF, 50 °C, **17** (59%) + **19** (39%); (g) 3 M NaOH, EtOH then 2 M HCl, 94%.

in an approximate 1:3 ratio. Acetylation of the mixture allowed separation of the respective acetates (*R*)- and (*S*)-**12** which were individually treated with sodium methoxide in methanol to give (*R*)- and (*S*)-**13**, the corresponding methyl ester derivatives of the original alcohols. The configuration at the newly formed stereogenic center in these products was tentatively assigned by NMR comparison with closely related diastereomeric pairs¹⁹ and the stereochemistry of the desired isomer (*S*)-**12** eventually confirmed in the tetrahydropyran derivatives **20** and **21** (vide infra). Alkene (*S*)-**13** was treated with *m*-CPBA and the resulting 2:1 mixture of epoxides exposed to sodium methoxide in methanol to give a product that exhibited partial ester hydrolysis. The crude material was therefore treated with TMS–diatomethane, following which chromatography afforded two fractions in an approximate ratio of 5:2, an unseparated mixture of two isomeric tetrahydropyrans **15**, and another component that was presumed to be a seven-membered ring isomer **16**. Silylation of the mixture of primary alcohols **15** gave **17**, C-pyranoside with an ‘ α -D-manno’ configuration and the ‘ β -L-gulo’ isomer **19** in a 3:2 ratio. The stereochemistry of **17** and **19** was assigned by ¹H NMR analysis of the acetylated derivatives **20** and **21**. Thus, the *J* values for the ring protons of **20** and the appearance of an NOE between H1 and H4 suggested a distorted chair-like conformation. This translates to *syn* relationships between H1 and H4 and H2 and H3, and confirms the configuration at C1 and C2, the two new stereogenic centers that were introduced in the reaction leading to (*S*)-**12**. Similarly, *J* data and an NOE between H1 and H5 pointed to the stereochemistry indicated in **21**. That the configuration at C1 in **20** and **21** was determined to be opposite is consistent with synthetic logic. Finally, saponification of **17** provided **18**, the required precursor for C-disaccharide **5**.

Thioacetal **6** and difluoro acid **18** were next subjected to the C-glycosidation sequence (Scheme 3). The Yamaguchi esterification procedure on **6** and **18** provided



Scheme 3. Synthesis of difluoro-C-disaccharide **5**. Reagents: (a) **18**, 2,4,6-trichlorobenzoyl chloride, Et₃N, THF then **6**, DMAP, toluene, 76% based on **18**; (b) Takai reagent, 63%; (c) MeOTf, DTBMP, CH₂Cl₂, MS 4A, 82%; (d) BH₃, Me₂S, THF; then Na₂O₂, 86%; (e) HCl in ether, CH₃OH, 63%; (f) Pd/C, HCOOH, CH₃OH, 93%.

ester **22** in 76% yield.²¹ Takai methylenation on **22** afforded the difluoro enol ether **23** in 63% yield based on recovered **22**.²² The reactivity of the difluoro ester and enol ether under acidic and basic conditions is noteworthy. Thus, the acid sensitivity of the methylene linked enol ethers that were prepared in our earlier study called for chromatography on basic alumina.¹⁶ While the difluoro derivative **23** was also stable under these conditions, it was discovered, during the purification of the mixture of **22** and **23**, that the α,α -difluoro ester was not. In comparison, both ester **22** and enol ether **23** were stable to chromatography on silica gel. The key cyclization reaction on **23** was promoted by methyl triflate in the presence of 2,6-di-*tert*-butyl-4-methylpyridine (DTBMP), giving the difluoromethylene linked glycal **24** in 82% yield. Thus, as initially feared, the difluoromethylene moiety did not have an adverse effect on the oxocarbenium ion cyclization. Hydroboration of **24** provided difluoromethylene linked C-disaccharide **25** as a single diastereomer in 86% yield. The straightforward removal of the alcohol protecting groups provided the title C-disaccharide **5**.

2.2. Conformational analysis

The potential energy surfaces for **5** was calculated using the MM3*²³ force field, as previously described (Fig. 2).^{12,24,25} These maps are useful to delimit the low-energy regions that are accessible to rotation around the glycosidic torsion angles Φ_{Gal} (H1_{Gal}–C1_{Gal}–X–C1_{Man}) and Φ_{Man} (H1_{Man}–C1_{Man}–X–C1_{Gal}). The different conformers have been dubbed, *exo*, *non-exo* and *anti* with respect to glyconic torsions Φ_{Gal} and Φ_{Man} , by analogy with the *exo*-anomeric notation for O-glycosides. Thus *exo*- Φ_{Gal} and *exo*- Φ_{Man} correspond to values of ca +60° and –60°, *non-exo*- Φ_{Gal} and *non-exo*- Φ_{Man} to –60° and +60°, and *anti*- Φ_{Gal} and *anti*-

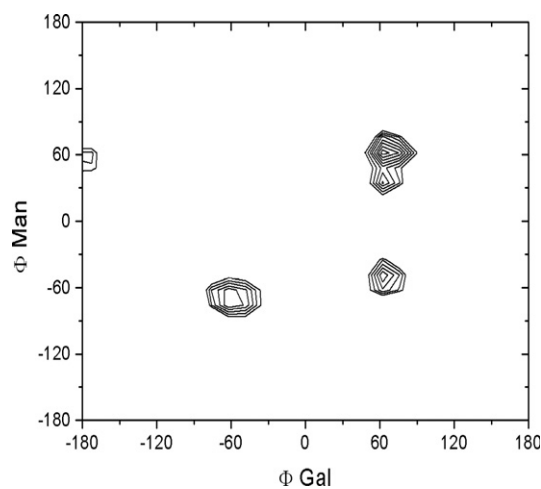


Figure 2. Steric energy map (Φ_{Man} , Φ_{Gal}) calculated by MM3* with $\epsilon = 80$ for **5**. Contours are given every 2.5 kJ mol^{-1} .

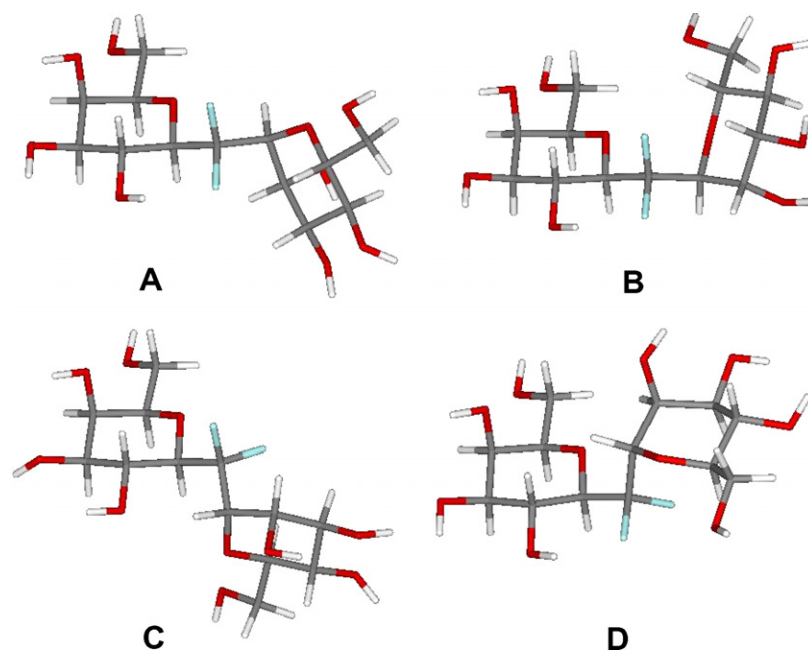


Figure 3. Stereoviews of the global and local minima A–D of **5** according to MM3* calculations. See Table 1 for Φ_{Gal} and Φ_{Man} for the different conformers.

Φ_{Man} to 180° , respectively. Four principal low-energy conformer types were obtained, but with very different populations: (A) *exo*- Φ_{Gal} /*non-exo*- Φ_{Man} , (B) *exo*- Φ_{Gal} /*exo*- Φ_{Man} , (C) *non-exo*- Φ_{Gal} /*exo*- Φ_{Man} , and (D) *anti*- Φ_{Gal} /*non-exo*- Φ_{Man} . These conformations are shown in Fig. 3, and their geometries and relative energies summarized in Table 1.

In addition, the conformational stability of the different conformers was checked by using MD simulations also with the MM3* force field.²⁶ Some of the computed $\Phi_{\text{Man}}/\Phi_{\text{Gal}}$ distributions are displayed in Figure 4.

Examination of the four different conformational families revealed several proton–proton distances of close to 2.5 Å that are unique to a particular conformation of **5**. An NOE corresponding to any of these proton pairs is deemed an exclusive NOE, and is diagnostic of a

specific conformation.²⁷ Exclusive NOEs are shown in bold in Table 1.

2.3. Experimental confirmation of modeling data by NMR

In order to deduce the final conformational distribution for **5**, the predictions from the force field calculations were compared with the experimental data as determined from NMR. The chemical shifts in D₂O are listed in Table 2. Assignment of resonances was made through a combination of COSY, TOCSY, 1D and 2D-NOESY/ROESY, and HSQC experiments.

The *J* values for the ring protons indicate that all the pyranose chairs adopt the usual ⁴C₁ chair (Table 2). The intermediate observed values for the C5–C6 lateral chains are in agreement with equilibria between the tg:gt

Table 1. Comparison between the inter-residue proton–proton distances calculated by MM3* for the conformers A–D (approximated Φ_{Gal} and Φ_{Man} angles in brackets), of **5** and the observed NOEs in the 1D-NOESY spectrum at 350 ms mixing time for **5**

Conformer ($\Phi_{\text{Gal}}/\Phi_{\text{Man}}$)	A(60/60) <i>exo/non-exo</i>	B(50/–50) <i>exo/exo</i>	C(–70/–70) <i>non-exo/exo</i>	D(–170/60) <i>anti/non-exo</i>	Ensemble average	Best fit A:B:C:D
ΔE (kJ/mol)	2.0	1.6	0	12.8		
Population (%)	22.5%	26.5%	50.7%	0.3%		25:15:50:10
	NOE exp (%)/distance (Å)	Calc distance (Å)	Calc distance (Å)	Calc distance (Å)	Calc distance (Å)	Ensemble average distance (Å)
1M–2M (internal reference)	4.7%/2.55 Å	2.55	2.55	2.55	2.55	
1G–1M	1.9%/3.0 Å	3.0	2.4	3.2	3.7	2.9
1G–2M	3.9%/2.6 Å	2.1	4.3	4.7	3.8	2.6
1G–5M	Overlap	4.5	4.2	2.5	4.5	—
1M–2G	1.7%/3.0 Å	4.3	4.7	3.2	2.2	3.0
2M–G2	<0.4%/>3.8 Å	4.9	5.2	4.8	2.7	3.8

In all cases, NOEs or ROEs were positive; that is, the cross peaks showed different sign to diagonal peaks, as expected for small molecules. Relative steric energies for (ΔE , kJ/mol) are also given. Interproton distances corresponding to exclusive NOEs are shown in bold.

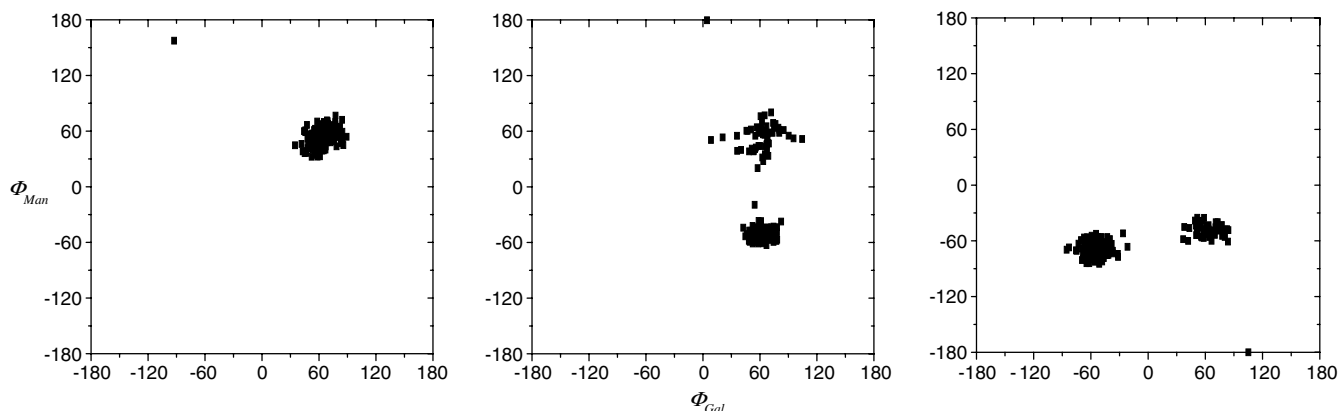


Figure 4. Frequency of sampling of $\phi_{\text{Man}}/\phi_{\text{Gal}}$ torsion angles from the MD simulations (MM3*) for **5**, starting from the different local minima. From left to right, starting from minima **A**, **B**, and **C**, respectively. Transitions from **B** to **A** (central panel) and from **C** to **B** (right panel) are observed.

Table 2. ^1H NMR chemical shifts (δ , ppm) and vicinal coupling constants (J , Hz) for compound **5**

Atom	δ , ppm (J , Hz)
H1M	4.51 (2.3, 14.3, 19.4)
H2M	4.33 (2.3, 3.4)
H3M	3.92 (3.8, 9.1)
H4M	3.62 (9.0, 9.0)
H5M	3.66 (9.0, 2.2, not meas.)
H6aM	3.89 (12.2)
H6bM	3.74
F1	(14.3, 14.3)
F2	(14.3, 19.4)
H1G	3.84 (14.3, 14.3, 10.0)
H2G	3.93 (9.8, 9.6)
H3G	3.70 (9.6, 3.4)
H4G	4.00 (3.4, 0.5)
H5G	3.79 (0.5, 3.5, 6.8)
H6aG	3.76
H6bG	3.74 (6.8, 12.2)

conformers for the Gal ring and the gg:gt conformers for the Man moiety.²⁸ The anomeric protons of both Gal and Man residues show scalar couplings to the fluorine atoms at the pseudoglycosidic linkage. The observed couplings vary between only 15 and 20 Hz, which are intermediate values for vicinal H/F arrangements. In previous studies, we have used the vicinal H/F couplings as additional data to assess the conformational equilibrium around the intersaccharide torsions.¹³ Unfortunately, it is well known that the presence of additional electronegative substituents along the coupling pathway strongly modify the relationship between torsion angles and coupling constants and, thus, the available Karplus-like equation for vicinal H/F couplings is not valid for this molecule. Therefore, the conformational analysis with respect to the intersaccharide linker has to rely exclusively on the NOE data.^{29,30} Accordingly, NOESY and ROESY experiments were carried out to determine the intensities of the observed NOEs. Experimental proton–proton distances were ob-

tained as described in the experimental section and compared to those estimated by the MM3* molecular mechanics and dynamics calculations (Table 1).

The ensemble averaged distances computed on the basis of the population ratios obtained from MM3* agree reasonably well with those experimentally deduced from the NOE values (see Section 4). Both sets of data support the presence of a conformational equilibrium among several conformers. However, some experimental distances are slightly different from those calculated from the MM3 distribution. Thus, the relative weakness of the 1Man–2Gal NOE and the very small intensity of 2Man–2Gal, which is exclusive for conformer **D**, indicates that a major contribution from conformer **D** is unlikely. However, the fact that this NOE is at all observed suggests that the 0.3% deduced from MM3* is underestimated. The presence of conformers **A** and **B** is also granted since the 1Gal–2Man and 1Gal–1Man NOEs are exclusive for these geometries. In this case the MM3* prediction appears to be somewhat high. The presence of the global minimum **C** is only grounded on the MM3* calculations and cannot be directly demonstrated by NMR because its exclusive NOE cannot be determined, due to overlapping between the two key protons (H1 Gal and H5 Man show the same chemical shift). Thus, although the experimental data was qualitatively consistent with the calculated trends, it was not definitive, as the experimental NOE values could also fit other population distributions. To examine this possibility, a systematic variation of the populations of the four conformers was then performed and the computed distances were compared to the experimental ones.³¹ Using this protocol, it was deduced that the relative percentages of the observable NOEs can only be accounted for when a significant population of **C** is considered. Attempts to fit all the observable NOEs (see Table 1) when minimum **C** was not considered did not succeed. In fact, the best fit to the experimental NOEs is obtained when a 25:15:50:10 distribution of **A**:**B**:**C**:**D**

is considered. Therefore, compound **5** exists predominantly as a conformational equilibrium between natural and *non-natural* conformers⁴ with substantial (ca. 50%) non-*exo*-anomeric conformations around the Φ_{Gal} glycosidic linkage, and detectable, ~35%, contribution of the non-*exo*-anomeric conformer for Φ_{Man} . Thus, overall, the MM3* simulations within MACROMODEL³² agree reasonably well with the observed populations.

3. Conclusion

As described in earlier studies, the conformational distributions around the glycosidic linkages of the parent O-glycoside **1** and its C-glycoside analogue, **2**, are rather different. The O-glycoside populates almost entirely (>93%) the natural *exo*-Gal/*exo*-Man (**B**) conformation, whereas the C-glycoside exists in this conformation in only 30%, with four other conformational families **A** (42%), **C** (6%), **D** (10%), and **E** (12%).¹² The monofluorinated analogue **3** shows a high preference for **A** (90%). The present investigation indicates that the difluoro-C-glycoside **5** populates the non-*exo*-Gal/*exo*-Man conformer **C** to a major extent (ca 50%), with additional contributions (~10–25%) from **A**, **B**, and **D**. Thus **5** might not be an accurate biological mimetic of the O-glycoside **1**, if the active conformation corresponds to the ground state of **1**. Difluoro-C-glycosides mimics like **5** could be more effective in cases where the glycosidic oxygen of the parent O-glycoside interacts directly with the receptor. This relative activity of **5** with respect to different carbohydrate receptors is an avenue for future investigation.

4. Experimental

4.1. Synthetic general methods

Unless otherwise stated, all reactions were carried out under a nitrogen atmosphere in oven-dried glassware using standard syringe and septa technique. ¹H and ¹³C NMR spectra were obtained on a Varian Unity Plus 500 (500 MHz) spectrometer. Chemical shifts are relative to the deuterated solvent peak or the tetramethylsilane (TMS) peak at (δ 0.00) and are in parts per million (ppm). Assignments for selected nuclei were determined from ¹H COSY experiments. High-resolution mass spectrometry (HRMS) was performed on an Ultima Micro-mass Q-ToF instrument at the Mass Spectrometry Laboratory of the University of Illinois, Urbana-Champaign. Thin layer chromatography (TLC) was done on 0.25 mm thick precoated silica gel HF₂₅₄ aluminum sheets. Chromatograms were observed under UV (short and long wavelength) light, and were visualized by heating plates that were dipped in a solution of ammo-

nium(VI) molybdate tetrahydrate (12.5 g) and cerium(IV) sulfate tetrahydrate (5.0 g) in 10% aqueous sulphuric acid (500 mL). Flash column chromatography (FCC) was performed using silica gel 60 (230–400 mesh) and employed a stepwise solvent polarity gradient, correlated with TLC mobility.

4.2. (3*S*) Ethyl 3-acetoxy-4,5,6-tris(benzyloxy)-2,2-difluorooct-7-enoate [(*S*)-**12**] and (3*R*) ethyl 3-acetoxy-4,5,6-tris(benzyloxy)-2,2-difluorooct-7-enoate [(*R*)-**12**]

To a solution of activated zinc dust (13.2 g, 0.21 mol) in dry THF at reflux (30 mL) was added ethyl bromodifluoroacetate (19.1 mL, 0.15 mol). After 10 min, a solution of **11**²⁰ (20.0 g, 0.05 mmol) in THF (60 mL) was introduced dropwise over 30 min. The mixture was then heated at reflux for 3 h, cooled to rt and carefully poured into 1 N HCl (40 mL) and ice (40 g), and extracted with EtOAc (3 × 150 mL). The organic layer was washed with saturated aqueous NaHCO₃, and brine, dried (Na₂SO₄), and concentrated in vacuo. FCC of the residue gave a mixture of epimeric alcohols (13.9 g, 54%) in a 3:1 ratio; colorless oil; R_f = 0.29 (10% EtOAc/petroleum ether); ¹H NMR (CDCl₃) δ 1.74 (t, J = 7.1 Hz, 2.3H), 1.32 (t, J = 7.1 Hz, 0.7H), 3.38 (dd, J = 3.2, 10.0 Hz, 0.3H), 3.58 (m, 0.7H) 3.77 (m, 0.3H), 3.86 (m, 1.7H), 3.94–4.08 (m, 1.7H), 4.11–4.22 (m, 0.7H), 4.31 (q, J = 7.1 Hz, 0.6H), 4.40–4.87 (m, 7H), 5.37–5.50 (m, 2H), 5.92 (m, 0.7H), 6.03 (m, 0.3H), 7.27–7.39 (m, 15H); ¹³C NMR (CDCl₃) major isomer: δ 13.8, 62.5, 70.4, 75.2, 78.9 (d, J = 3.9 Hz), 81.6, 82.9, 114.8 (dd, J = 257.3, 257.4 Hz), 120.0, 127.9, 128.1–128.6 (several resonances), 135.3, 137.4, 138.01, 138.4, 163.4 (t, J = 30.8 Hz). Minor isomer: δ 14.0, 63.2, 70.4, 70.6, 73.9 (d, J = 3.4 Hz), 74.3, 75.3, 80.0, 81.7, 119.5, 127.0–129.0 (several resonances) 135.8, 137.6, 137.99, 138.2, 163.6 (dd, J = 30.0, 33.1 Hz). ESIMS calcd for C₃₁H₃₈O₆F₂N [M+NH₄]⁺: 558.2662. Found: 558.2651.

A portion of the above mixture (0.52 g, 1.09 mmol) was dissolved in EtOAc (30 mL) and treated with acetic anhydride (0.52 mL, 5.45 mmol) and DMAP (26.6 mg, 0.22 mmol) for 30 min. MeOH (1 mL) was added and the volatiles were removed under reduced pressure. FCC of the residue afforded (*S*)-**12** (0.40 g, 64%) and (*R*)-**12** (0.13 g, 21%) as colorless oils.

For (*S*)-**12**: R_f = 0.38 (10% EtOAc/petroleum ether); [α]_D –21.0 (c 1.5, CHCl₃); IR (film) 1767 (s) cm^{–1}; ¹H NMR (CDCl₃) δ 1.08 (t, J = 7.1 Hz, 3H), 2.20 (s, 3H), 3.74 (d, J = 8.1 Hz, 1H), 3.92 (q, J = 7.1 Hz, 1H), 4.06 (m, 3H), 4.41 (A of ABq, J = 10.8 Hz, $\Delta\delta$ = 0.15 ppm, 1H), 4.44 (A of ABq, J = 12.2 Hz, $\Delta\delta$ = 0.25 ppm, 1H), 4.56 (B of ABq, J = 10.8 Hz, $\Delta\delta$ = 0.15 ppm, 1H), 4.68 (B of ABq, J = 12.2 Hz, $\Delta\delta$ = 0.25 ppm, 1H), 4.87 (ABq, J = 12.0 Hz, $\Delta\delta$ = 0.04 ppm, 2H), 5.39 (d, J = 17.1 Hz, 1H), 5.46 (dd, J = 1.2,

10.5 Hz, 1H), 5.81 (ddd, $J = 7.8, 10.5, 17.4$ Hz, 1H), 6.00 (ddd, $J = 3.2, 10.5, 20.8$ Hz, 1H), 7.19–7.44 (m, 15H); ^{13}C NMR (CDCl_3) δ 13.7, 20.6, 62.8, 69.4 (t, $J = 22.0$ Hz), 70.5, 73.0, 75.0, 77.3 (d, $J = 2.7$ Hz), 81.2, 81.8, 113.3 (dd, $J = 251.1, 257.5$ Hz), 120.4, 127.9–128.7 (several resonances), 135.0, 137.1, 138.4, 138.8, 162.3 (dd, $J = 28.9, 33.1$ Hz), 168.4. ESIMS calcd for $\text{C}_{33}\text{H}_{40}\text{O}_7\text{F}_2\text{N} [\text{M}+\text{NH}_4]^+$: 600.2767. Found: 600.2761.

For (*R*)-**12**: $R_f = 0.28$ (10% EtOAc/petroleum ether); ^1H NMR (CDCl_3) δ 1.23 (t, $J = 7.1$ Hz, 3H), 2.07 (s, 3H), 3.78 (dd, $J = 4.2, 6.5$ Hz, 1H), 4.20 (m, 4H), 4.38–4.25 (m, 2H), 4.64–4.80 (m, 4H), 5.42 (d, $J = 10.4$ Hz, 1H), 5.48 (d, $J = 17.3$ Hz, 1H), 5.80 (ddd, $J = 2.2, 12.7, 19.9$ Hz, 1H), 6.01 (ddd, $J = 7.8, 10.4, 17.6$ Hz, 1H), 7.28–7.43 (m, 15H); ^{13}C NMR (CDCl_3) δ 13.9, 20.7, 63.3, 70.0 (dd, $J = 24.6, 28.6$ Hz), 73.2, 74.2, 75.1, 80.6, 81.8, 113.2 (dd, $J = 255.2, 257.4$ Hz), 119.4, 127.7–128.5 (several resonances), 135.9, 138.1, 138.4, 138.5, 162.8 (dd, $J = 30.3, 32.9$ Hz), 168.5. ESIMS calcd for $\text{C}_{33}\text{H}_{40}\text{O}_7\text{F}_2\text{N} [\text{M}+\text{NH}_4]^+$: 600.2767. Found: 600.2753.

4.3. (3*S*)-Methyl 4,5,6-tris(benzyloxy)-2,2-difluoroct-7-enoate (*S*)-**13**

A solution of ethyl ester-acetate (*S*)-**12** (1.11 g, 1.90 mmol) in dry MeOH (20 mL) was treated with 1 M MeONa in MeOH (5.7 mL, 5.7 mmol). After stirring for 1 h at rt, the reaction was neutralized with 2 N HCl and the solvent evaporated under reduced pressure. FCC of the residue afforded (*S*)-**13** (0.79 g, 83%) as a colorless oil; $R_f = 0.54$, (10% EtOAc/petroleum ether); ^1H NMR (CDCl_3) δ 3.50 (s, 3H), 3.52 (m, 1H), 3.84 (m, 2H), 4.11 (t, $J = 7.1$ Hz, 1H), 4.36–4.73 (m, 5H), 4.83 (s, 2H), 5.37 (d, $J = 18.6$ Hz, 1H), 5.41 (d, $J = 18.6$ Hz, 1H), 5.90 (ddd, $J = 8.3, 10.0, 17.6$ Hz, 1H), 7.14–7.46 (m, 15H); ^{13}C NMR (CDCl_3) δ 52.9, 70.7 (t, $J = 22.9$ Hz), 70.8, 72.9, 75.3, 77.3 (d, $J = 2.7$ Hz), 81.2, 81.8, 113.3 (dd, $J = 251.1, 257.5$ Hz), 120.4, 127.9–128.7 (several resonances), 135.0, 137.1, 138.4, 138.8, 163.8 (dd, $J = 30.2, 32.1$ Hz). ESIMS calcd for $\text{C}_{30}\text{H}_{36}\text{O}_6\text{F}_2\text{N} [\text{M}+\text{NH}_4]^+$: 544.2505. Found: 544.2505.

4.4. Epoxide mixture **14**

To a solution of (*S*)-**13** (0.79 g, 1.50 mmol) in CH_2Cl_2 (20 mL) was added a mixture of *m*-CPBA (2.61 g, 15.1 mmol), CH_2Cl_2 (20 mL), NaH_2PO_4 (4.30 g, 30.3 mmol), Na_2HPO_4 (4.14 g, 30.0 mmol) and water (40 mL). The suspension was stirred for 26 h at rt then poured into 10% Na_2SO_3 in saturated aqueous NaHCO_3 . After stirring for 1 h, the organic layer was separated, washed with brine, dried (Na_2SO_4) and evaporated under reduced pressure. FCC of the residue afforded **14** (0.50 g, 74% based on recovered alkene) as a 2:1 mixture; clear oil; $R_f = 0.30$ (15% EtOAc/petroleum

ether); ^1H NMR (CDCl_3) δ 2.47 (dd, $J = 2.7, 4.9$ Hz, 0.6H), 2.60 (t, $J = 4.5$ Hz, 0.6H), 2.68 (dd, $J = 2.6, 4.9$ Hz, 0.4H), 2.84 (t, $J = 4.6$ Hz, 0.4H), 3.09 (m, 0.4H), 3.36 (m, 0.6H), 3.30 (m, 0.6H), 3.53–3.60 (m, 3.8H), 3.68 (m, 0.6H), 3.91 (m, 1.6H), 4.01 (d, $J = 5.9$ Hz, 0.4H), 4.45–4.90 (m, 7H), 7.18–7.40 (m, 15H); ^{13}C NMR (CDCl_3) major isomer: δ 43.9, 52.7, 53.1, 70.6 (t, $J = 22.5$ Hz), 73.9, 74.4, 78.9 (d, $J = 3.3$ Hz), 80.8, 80.9, 114.9 (dd, $J = 250.0, 258.1$ Hz), 122.9–128.7 (several resonances), 137.4, 137.9, 138.1, 138.4, 138.8, 163.8 (dd, $J = 30.2, 32.3$ Hz). Minor isomer: δ 47.2, 51.1, 53.0, 70.1 (t, $J = 25.1$ Hz), 73.4, 75.2, 78.8 (d, $J = 3.4$ Hz), 79.5, 81.5, 115.0, (dd, $J = 250.0, 256.9$ Hz), 137.2, 137.7, 138.3, 163.7 (t, $J = 31.3$ Hz). ESIMS calcd for $\text{C}_{30}\text{H}_{36}\text{O}_7\text{F}_2\text{N} [\text{M}+\text{NH}_4]^+$: 560.2454. Found: 560.2452.

4.5. Methyl 3,7-anhydro-4,5,6-tri-*O*-benzyl-2,2-difluoro-*D*-glycero-*D*-talo-octosonate and methyl 3,7-anhydro-4,5,6-tri-*O*-benzyl-2,2-difluoro-*L*-glycero-*D*-talo-octosonate (**15**)

A solution of **14** (4.19 g, 7.73 mmol) in dry MeOH (400 mL) was treated with 1 M MeONa in MeOH (23.2 mL, 23.2 mmol). After stirring for 23 h at rt, the reaction was acidified to pH 2 with a solution of HCl in ether and the solvent evaporated under reduced pressure. The residue was dissolved in MeOH (20 mL) and toluene (60 mL) then treated with TMSCHN₂ (5.8 mL, 11.6 mmol, 2 M solution in ether) at 0 °C. After 30 min, acetic acid (1 mL) was added to the reaction and the volatiles were removed under reduced pressure. FCC of the residue yielded **15** (2.16 g, 52%), as an inseparable mixture, and **16** (0.95 g, 22%).

For **15**: colorless oil, $R_f = 0.49$ (30% EtOAc/petroleum ether); ^1H NMR (CDCl_3) δ 1.66 (d, $J = 8.9$ Hz, D_2O exchange, 0.5H), 1.87 (t, $J = 6.2$ Hz, D_2O exchange, 0.5H), 3.42 (dd, $J = 1.2, 3.3$ Hz, 0.5H), 3.50 (m, 0.5H), 3.65 (m, 2H), 3.75–3.98 (m, 5.5H), 4.08 (dd, $J = 3.2, 5.2$ Hz, 0.5H), 4.28–4.72 (m, 7H), 7.15–7.38 (m, 15H); ^{13}C NMR (CDCl_3) δ 53.0, 53.4, 61.7, 62.0, 71.4, 71.9, 72.0, 72.4, 72.5, 72.7–73.2 (several resonances), 73.4, 74.3, 74.8, 75.7, 76.9, 114.0 (t, $J = 254.7$ Hz), 114.9 (dd, $J = 256.3, 260.3$ Hz), 127.7–128.6 (several resonances), 137.4, 137.6, 137.9, 138.0, 163.37 (t, $J = 30.9$ Hz), 163.40 (dd, $J = 27.0, 31.8$ Hz). ESIMS calcd for $\text{C}_{30}\text{H}_{36}\text{O}_7\text{F}_2\text{N} [\text{M}+\text{NH}_4]^+$: 560.2454. Found: 560.2489.

For **16**: colorless oil, $R_f = 0.60$ (30% EtOAc/petroleum ether); ^1H NMR (CDCl_3) δ 3.13 (d, $J = 8.3$ Hz, D_2O exchange, 1H), 3.62 (s, 3H), 3.71 (m, 1H), 3.77 (dd, $J = 4.9, 12.6$ Hz, 1H), 3.83 (t, $J = 5.2, 1H$), 4.02 (d, $J = 6.0$ Hz, 1H), 4.06 (d, $J = 12.7$ Hz, 1H), 4.33–4.44 (m, 4H), 4.60 (s, 2H), 4.70 (ABq, $J = 11.8$ Hz, $\Delta\delta = 0.03$ ppm, 2H), 7.25–7.37 (m, 15H); ^{13}C NMR (CDCl_3) δ 53.3, 66.5, 67.2, 72.0, 72.5, 73.3, 74.1, 75.2, 80.1, 115.7 (t, $J = 255.7$ Hz), 127.1–128.8 (several reso-

nances), 137.5, 137.7, 138.0, 163.8 (t, $J = 31.5$ Hz). ESIMS calcd for $C_{30}H_{36}O_7F_2N$ $[M+NH_4]^+$: 560.2454. Found: 560.2451.

4.6. Methyl 3,7-anhydro-4,5,6-tri-*O*-benzyl-8-*O*-*t*-butyldiphenylsilyl-2,2-difluoro-*D*-glycero-*D*-talo-octosonate (17) and methyl 3,7-anhydro-4,5,6-tri-*O*-benzyl-8-*O*-*t*-butyldiphenylsilyl-2,2-difluoro-*L*-glycero-*D*-talo-octosonate (19)

The mixture of **15** (213 mg, 0.39 mmol), TBDPSCI (0.03 mL, 1.18 mmol), and imidazole (106 mg, 1.56 mmol) in anhydrous DMF (5 mL) was stirred at 50 °C for 2.5 h. The reaction was then quenched by the addition of MeOH (1 mL) and extracted with ether. The combined organic phase was washed with brine, dried (Na_2SO_4), filtered, and evaporated under reduced pressure. The residue was purified by gravity column chromatography to give **17** (180 mg, 59%) and **19** (119 mg, 39%).

For **17**: colorless oil, $R_f = 0.68$ (10% EtOAc/petroleum ether); IR (film) 1770 (s) cm^{-1} ; 1H NMR ($CDCl_3$) δ 1.11 (s, 9H), 3.69 (s, 3H), 3.91 (dd, $J = 6.4, 12.5$ Hz, 1H), 3.94–4.00 (m, 3H), 4.07 (t, $J = 5.9$ Hz, 1H), 4.13 (dd, $J = 3.2, 5.6$ Hz, 1H), 4.51 (dd, $J = 5.6, 10.5, 19.0$ Hz, 1H), 4.60–4.71 (m, 6H), 7.26 (m, 2H), 7.34–7.50 (m, 19H), 7.72 (m, 4H); ^{13}C NMR ($CDCl_3$) δ 26.9, 53.4, 62.8, 72.3, 72.87, 72.94 (dd, $J = 22.3, 27.0$ Hz), 73.5, 74.1, 77.4, 115.2 (dd, $J = 256.5, 258.8$ Hz), 127.8–129.8 (several resonances), 133.5, 133.8, 135.8, 136.0, 137.9, 138.3, 138.4, 163.6 (t, $J = 31.4$ Hz). ESIMS calcd for $C_{46}H_{54}O_7SiF_2N$ $[M+NH_4]^+$: 798.3632. Found: 798.3637.

For **19**: colorless oil, $R_f = 0.62$ (10% EtOAc/petroleum ether); 1H NMR ($CDCl_3$) δ 1.09 (s, 9H), 3.61 (s, 3H), 3.67 (dd, $J = 1.1, 3.7$ Hz, 1H), 3.75 (t, $J = 2.7$ Hz, 1H), 3.81 (m, 2H), 3.96 (dd, $J = 2.6, 10.0$ Hz, 1H), 4.03 (t, $J = 6.8$ Hz, 1H), 4.32–4.70 (m, 5H), 4.48 (A of ABq, $J = 12.1$ Hz, $\Delta\delta = 0.21$ ppm, 1H), 4.69 (B of ABq, $J = 12.1$ Hz, $\Delta\delta = 0.21$ ppm, 1H), 7.16 (m, 2H), 7.28–7.47 (m, 19H), 7.67 (m, 4H); ^{13}C NMR ($CDCl_3$) δ 27.0, 53.2, 62.3, 72.0, 72.1, 73.1, 73.2, 73.4 (two resonances, a singlet and an apparent t, $J = 23.0$ Hz), 74.8, 75.7, 114.3 (t, $J = 254.5$ Hz), 127.9–128.8 (several resonances), 133.4, 133.7, 135.7, 135.8, 137.8, 138.4 (two resonances), 163.7 (t, $J = 31.3$ Hz). ESIMS calcd for $C_{46}H_{54}O_7SiF_2N$ $[M+NH_4]^+$: 798.3632. Found: 798.3630.

4.7. 3,7-Anhydro-4,5,6-tri-*O*-benzyl-8-*O*-*t*-butyldiphenylsilyl-2,2-difluoro-*D*-glycero-*D*-talo-octosonic acid (18)

Methyl ester **17** (1.70 g, 2.18 mmol) was treated with a mixture of 3 N NaOH (2.2 mL, 6.54 mmol) and ethanol (40 mL). After 1 h the reaction mixture was concentrated in vacuo and acidified with 2 N HCl (20 mL). The mixture was then extracted with EtOAc and the

organic phase washed with water, dried (Na_2SO_4) and evaporated under reduced pressure to provide **18** (1.60 g, 94%); colorless oil, $R_f = 0.34$ (20% MeOH/ $CHCl_3$); 1H NMR ($CDCl_3$) δ 1.05 (s, 9H, $(CH_3)_3CSi$), 3.87–4.05 (m, 5H, H-4, 6, 7, 8a, 8b), 4.14 (dd, $J = 2.9, 6.2$ Hz, 1H, H-5), 4.48–4.66 (m, 7H, H-3, $3 \times PhCH_2$), 7.24–7.48 (m, 21H, Ph), 7.71 (m, 4H, Ph); ^{13}C NMR ($CDCl_3$) δ 27.0, 27.2 ($(CH_3)_3CSi$), 62.6 (C-8), 72.1 (t, $J = 24.1$ Hz) (C-4), 72.37, 72.43, 72.9, 73.1, 73.8, 76.2, 77.5 (7C, C-4, 5, 6, $3 \times PhCH_2$), 114.6 (t, $J = 257.0$ Hz) (C-2), 127.7–129.9 (several resonances), 133.4, 133.6, 135.8, 135.9, 137.6, 138.0, 138.2 (Ph), 166.4 (t, $J = 31.7$ Hz) (C-1). ESIMS calcd for $C_{45}H_{52}O_7SiF_2N$ $[M+NH_4]^+$: 784.3476. Found: 784.3464.

4.8. Methyl 4,5,6-tri-*O*-acetyl-3,7-anhydro-8-*O*-*t*-butyldiphenylsilyl-2,2-difluoro-*D*-glycero-*D*-talo-octosonate (20)

Colorless oil; $R_f = 0.44$ (30% EtOAc/petroleum ether); 1H NMR ($CDCl_3$) δ 1.08 (s, 9H, $(CH_3)_3-$), 1.99, 2.00, 2.12 (all s, 9H, $CH_3CO \times 3$), 3.71 (dd, $J = 3.2, 11.7$ Hz, 1H, H-6a), 3.75 (dd, $J = 4.7, 11.7$ Hz, 1H, H-6b), 3.82 (s, 3H, CH_3O-), 3.98 (m, 1H, H-5), 4.42 (ddd, $J = 3.6, 6.6, 23.4$ Hz, 1H, H-1), 5.38 (dd, $J = 3.6, 8.3$ Hz, 1H, H-3), 5.43 (t, $J = 8.3$ Hz, 1H, H-4), 5.65 (t, $J = 3.4$ Hz, 1H, H-2), 7.36–7.42 (m, 6H), 7.64–7.71 (m, 4H); ^{13}C NMR ($CDCl_3$) δ 20.8 (two resonances), 20.9, 26.9, 53.9, 62.5, 65.7, 66.1, 69.4 (d, $J = 4.3$ Hz), 74.3 (dd, $J = 22.0, 30.0$ Hz), 76.4, 114.5 (dd, $J = 258.1, 262.1$ Hz), 127.9 (two resonances), 128.5, 130.0, 133.2, 133.4, 135.8, 135.9, 162.9 (dd, $J = 29.2, 32.7$ Hz), 169.5, 169.7, 169.9. ESIMS calcd for $C_{31}H_{42}O_{10}SiF_2N$ $[M+NH_4]^+$: 654.2541. Found: 654.2537.

4.9. Methyl 4,5,6,8-tetra-*O*-acetyl-3,7-anhydro-2,2-difluoro-*L*-glycero-*D*-talo-octosonate (21)

Colorless oil; $R_f = 0.42$ (40% EtOAc/petroleum ether); 1H NMR (C_6D_6) δ 1.98, 2.06, 2.20 (all s, 12H, $CH_3CO \times 4$), 3.91 (s, 3H, CH_3O-), 4.14–4.16 (m, 2H, H-5, 6a), 4.17 (t, $J = 5.9$ Hz, 1H, H-6b), 4.34 (ddd, $J = 7.8, 8.3, 14.4$ Hz, 1H, H-1), 5.00 (dd, $J = 1.5, 3.9$ Hz, 1H, H-4), 5.40 (dd, $J = 3.2, 10.3$ Hz, 1H, H-2), 5.43 (t, $J = 3.2$ Hz, 1H, H-3); ^{13}C NMR ($CDCl_3$) δ 20.6, 20.8, 20.9 (two resonances), 53.6, 61.9, 63.9 (d, $J = 4.2$ Hz), 66.6, 67.8, 72.9 (dd, $J = 23.8, 28.4$ Hz), 73.0, 113.6 (dd, $J = 252.0, 261.5$ Hz), 163.2 (dd, $J = 30.2, 32.2$ Hz), 169.0 (two resonances), 169.7, 170.5. ESIMS calcd for $C_{17}H_{26}O_{11}F_2N$ $[M+NH_4]^+$: 458.1468. Found: 458.1467.

4.10. Ester (22)

A mixture of acid **18** (43 mg, 0.06 mmol), 2,4,6-trichlorobenzoyl chloride (0.01 mL, 0.06 mmol) and triethyl-

amine (0.02 mL, 0.12 mmol) in THF (3 mL) was stirred for 3.5 h at 0 °C. DMAP (10.0 mg, 0.08 mmol) and a solution of alcohol **6** (31 mg, 0.06 mmol) in toluene was added, and stirring continued for 1 h. The mixture was then diluted with ether (10 mL), washed with saturated aqueous NaHCO₃ and brine, dried (Na₂SO₄), filtered, and evaporated under reduced pressure. The residue was purified by FCC to give ester **22** (54 mg, 91% based on recovered **6**, 76% based on consumed **18**); colorless oil; *R*_f = 0.33 (10% EtOAc/petroleum ether); [α]_D -32.2 (*c* 1.0, CHCl₃); IR (film) 1780 (s) cm⁻¹; ¹H NMR (CDCl₃) δ 1.04 (two singlets, 18H, 2 × (CH₃)₃CSi), 1.31, 1.43, (both s, 6H, C(CH₃)₂), 3.77–3.89 (m, 5H, H-4'a, 4'b, 5, 8a, 8b), 3.91 (q, *J* = 5.1 Hz, 1H, H-7), 3.99 (t, *J* = 5.9 Hz, 1H, H-6), 4.07 (dd, *J* = 3.0, 5.6 Hz, 1H, H-4), 4.39–4.60 (m, 8H, H-2', 3, 3 × PhCH₂), 5.22 (m, 1H, H-3'), 5.42 (d, *J* = 6.6 Hz, 1H, H-1'), 7.16–7.42 (m, 30H, Ph), 7.52 (m, 2H, Ph), 7.65 (m, 8H, Ph); ¹³C NMR (CDCl₃) δ 26.7, 26.9, 27.0, 27.2, 61.6, 62.8, 72.5, 72.6, 72.7, 72.9, 73.2, 74.0, 74.5, 77.1, 77.6, 78.7, 84.7, 112.1, 114.9 (t, *J* = 257.4 Hz), 127.8–129.8 (several resonances), 130.0, 132.6, 132.9, 133.0, 133.4, 133.5, 133.8, 135.8 (three resonances), 135.9, 136.0, 137.8, 138.4, 138.5, 162.4 (t, *J* = 31.8 Hz). ESIMS calcd for C₇₄H₈₆O₁₀SSi₂F₂N [M+NH₄]⁺: 1274.5474. Found: 1274.5476.

4.11. Enol ether (**23**)

TMEDA (1.20 mL, 7.96 mmol) was added at 0 °C to a mixture of 1 M titanium tetrachloride in CH₂Cl₂ (4.98 mL, 4.98 mmol) and THF (6 mL). The resulting yellow-brown suspension was allowed to warm to rt and stirred for 30 min. At this point freshly activated zinc dust (546 mg, 8.36 mmol) and lead(II) chloride (28 mg, 0.10 mmol) were added in one portion and stirring was continued for 10 min. To the resulting bluish-green mixture was added a solution of ester **22** (257 mg, 0.20 mmol) and dibromomethane (0.28 mL, 3.98 mmol) in THF (6 mL). The mixture was stirred at 60 °C for 3.5 h then diluted with brine, and cooled to rt over 30 min. Ether (20 mL) was then added and vigorous stirring continued for 20 min. The suspension was filtered through neutral alumina and the residue washed with ether. The ethereal extract was concentrated in vacuo and gravity chromatography of the residue over silica gel afforded enol ether **23** (101 mg, 63%, based on recovered **22**); colorless oil; *R*_f = 0.53 (5% EtOAc/petroleum ether); ¹H NMR (C₆D₆) δ 1.15, 1.17 (both s, 18H, 2 × (CH₃)₃CSi), 1.47, 1.55, (both s, 6H, C(CH₃)₂), 3.81 (dd, *J* = 5.9, 11.0 Hz, 1H, H-8a), 4.01–4.15 (m, 5H, H-3', 4'a, 6, 7, 8b), 4.18 (dd, *J* = 7.3, 11.0 Hz, 1H, H-4'b), 4.31 (apparent t, *J* = 2.5 Hz, 1H, H-6), 4.35 (t, *J* = 3.7 Hz, 1H, H-9a), 4.43–4.49 (m, 4H, H-4, 3 × PhCH), 4.62 (A of ABq, *J* = 11.9 Hz, Δδ = 0.14 ppm, 1H, PhCH), 4.69 (B of ABq, *J* = 11.9 Hz,

Δδ = 0.14 ppm, 1H, PhCH), 4.75 (d, *J* = 3.7 Hz, 1H, H-9b), 4.79 (dd, *J* = 2.7, 5.6 Hz, 1H, H-2'), 4.87 (d, *J* = 11.3 Hz, 1H, PhCH), 5.08 (ddd, *J* = 1.7, 7.6, 26.7 Hz, 1H, H-1), 6.22 (d, *J* = 5.6 Hz, 1H, H-1'), 6.89–7.43 (m, 30H, Ph), 7.65–7.88 (m, 10H, Ph); ¹³C NMR (C₆D₆) δ 27.3, 27.4, 27.6, 27.9, 62.1, 65.2, 72.6, 73.0, 73.5, 74.7 (dd, *J* = 22.0, 32.1 Hz), 75.0, 75.2, 78.9 (d, *J* = 4.6 Hz), 81.0, 84.9, 88.3 (t, *J* = 4.6 Hz), 113.1, 119.8 (dd, *J* = 248.4, 253.9 Hz), 127.3–129.5 (several resonances), 130.2 (two resonances), 130.6 (two resonances), 131.6, 133.6, 133.8, 134.5, 134.6, 135.5, 136.4, 136.5, 139.1, 139.5, 139.7, 154.3 (dd, *J* = 23.8, 31.2 Hz). ESIMS calcd for C₇₅H₈₈O₉SSi₂F₂N [M+NH₄]⁺: 1272.5681. Found: 1272.5671.

4.12. Glycal (**24**)

Enol ether **23** (200 mg, 0.16 mmol), 2,6-di-*tert*-butyl-4-methylpyridine (163 mg, 1.59 mmol), and freshly activated, powdered 4A molecular sieves (400 mg) in anhydrous CH₂Cl₂ (15 mL) were stirred for 15 min at rt under an argon atmosphere and then cooled to 0 °C. Methyl triflate (0.18 mL, 0.80 mmol) was then introduced, and the mixture was warmed to rt and stirred for an additional 2 d, at which time triethylamine (0.2 mL) was added. The mixture was diluted with ether, washed with saturated aqueous NaHCO₃ and brine, dried (Na₂SO₄), filtered and evaporated under reduced pressure. The residue was purified by FCC to give glycal **24** (124 mg, 82% based on recovered **23**), clear oil, *R*_f = 0.54 (10% EtOAc/petroleum ether); ¹H NMR (C₆D₆) δ 1.16, 1.18 (both s, 18H), 1.27, 1.28, (both s, 6H), 3.86 (t, *J* = 6.9 Hz, 1H), 4.03–4.17 (m, 7H), 4.30 (t, *J* = 2.9 Hz, 1H), 4.38 (m, 1H), 4.50–4.60 (m, 5H), 4.72 (A of ABq, *J* = 11.5 Hz, Δδ = 0.23 ppm, 1H), 4.79 (apparent ddd, *J* = 2.9, 10.0, 22.7 Hz, 1H), 4.98 (B of ABq, *J* = 11.5 Hz, Δδ = 0.23 ppm, 1H), 5.41 (d, *J* = 2.7 Hz, 1H), 7.08–7.38 (m, 27H), 7.70–7.87 (m, 8H); ¹³C NMR (C₆D₆) δ 27.4, 27.5, 28.8, 63.7, 63.8, 69.3, 72.2, 73.0, 73.3, 74.0, 74.9, 75.2 (dd, *J* = 24.7, 30.2 Hz), 77.5, 78.5, 80.3 (d, *J* = 2.7 Hz), 102.7 (t, *J* = 5.5 Hz), 111.3, 118.8 (dd, *J* = 247.4, 252.0 Hz), 127.9–128.9 (several resonances), 133.9, 134.1 (two resonances), 136.2, 136.3, 136.4, 136.7, 139.2, 139.5, 139.9, 148.5 (dd, *J* = 26.6, 31.2 Hz). ESIMS calcd for C₆₉H₈₂O₉Si₂F₂N [M+NH₄]⁺: 1162.5491. Found: 1162.5497.

4.13. 2,6:8,12-Dianhydro-9,10,11-tri-*O*-benzyl-1,13-di-*O*-*tert*-butyldiphenylsilyl-3,4-*O*-isopropylidene-7-deoxy-7,7-difluoro-*D*-erythro-*L*-allo-*L*-galacto-tridecitol (**25**)

Borane dimethyl sulfide complex (0.11 mL, 1.10 mmol) was added at 0 °C to a solution of glycal **24** (0.12 g, 0.11 mmol) in anhydrous THF (10 mL) under an atmosphere of argon. The mixture was warmed to rt and stirred for an additional 2 h at this temperature. The

solution was then cooled to 0 °C and treated with a mixture of 3 N NaOH (6 mL) and 30% aqueous H₂O₂ (6 mL) for 30 min. The mixture was diluted with ether, washed with saturated aqueous NaHCO₃ and brine, dried (Na₂SO₄), filtered and evaporated under reduced pressure. The residue was purified by FCC to give **25** (0.11 g, 86%) as a colorless oil; $R_f = 0.48$ (20% EtOAc/petroleum ether); IR (film) 3441 (m) cm⁻¹; ¹H NMR (CDCl₃) δ 1.07 (s, 18H, 2 × (CH₃)₃CSi), 1.35, 1.47, (both s, 6H, C(CH₃)₂), 2.93 (d, $J = 5.3$ Hz, 1H, D₂O exchange, -OH), 3.54 (m, 1H, H-1'), 3.68 (t, $J = 7.6$ Hz, 1H, H-4), 3.79 (ddd, $J = 2.2, 6.1, 7.8$ Hz, 1H, H-5'), 3.80–3.97 (m, 8H, H-2', 3', 6'a, 6'b, 3, 5, 6a, 6b), 4.09 (t, $J = 3.4$ Hz, 1H, H-2), 4.27 (dd, $J = 2.5, 5.1$ Hz, 1H, H-4'), 4.36 (d, $J = 11.3$ Hz, 1H, PhCH), 4.50–4.62 (m, 6H, H-1, 5 × PhCH), 7.06 (m, 2H, Ph), 7.22–7.42 (m, 25H, Ph), 7.65–7.73 (m, 8H, Ph); ¹³C NMR (CDCl₃) δ 26.5, 27.0, 27.3, 28.5, 62.7, 64.3, 69.7, 72.8 (two resonances), 72.9, 73.4, 74.0, 74.5, 76.6 (apparent t, $J = 31.9$ Hz), 78.2, 78.7, 80.2, 109.9, 121.2 (t, $J = 254.2$ Hz), 127.8–130.0 (several resonances), 133.2, 133.5, 133.7, 135.8, 135.9, 136.0, 138.2, 138.3, 138.5. ESIMS calcd for C₆₉H₈₄O₁₀-Si₂F₂N [M+NH₄]⁺: 1180.5596. Found: 1180.5601.

4.14. 2,6:8,12-Dianhydro-7-deoxy-7,7-difluoro-D-erythro-L-*allo*-L-galacto-tridecitol (5)

A saturated solution of HCl in ether (0.2 mL) was added to a solution of C-glycoside **25** (87 mg, 0.07 mmol) in anhydrous MeOH (8.0 mL) to a pH of 4. The mixture was stirred at rt and after 2.5 h, the volatiles were removed under reduced pressure. FCC of the crude residue provided the pentol derivative resulting from removal of the acetal and silyl ether protecting groups (30 mg, 63% yield): $R_f = 0.28$ (95% EtOAc/petroleum ether); ¹H NMR (CDCl₃) δ 2.24 (br s, D₂O exchange, 2H), 3.41 (s, 2H), 3.53 (m, 2H), 3.70 (m, 3H), 3.79 (m, 1H), 3.85 (t, $J = 9.5$ Hz, 1H), 3.96 (apparent t, $J = 5.0$ Hz, 1H), 4.02 (s, 1H), 4.11 (m, 2H), 4.38–4.61 (m, 7H), 4.84 (br s, 1H), 7.17–7.33 (m, 15H). ESIMS calcd for C₃₄H₄₀O₁₀F₂Na [M+Na]⁺: 669.2482. Found: 669.2480.

A mixture of material from the previous step (12 mg, 0.02 mmol), 10% Pd-C (30 mg), formic acid (0.05 mL) and CH₃OH (3 mL) was stirred under an atmosphere of hydrogen (balloon) for 18 h. The reaction mixture was then purged with argon, filtered through a bed of Celite and the filtrate concentrated under reduced pressure to give **5** (8 mg, 93%) as a colorless oil; $R_f = 0.32$ (50% MeOH/CH₃Cl); $[\alpha]_D^{25} +25.1$ (c 0.75, H₂O); ¹H NMR (see Table 2); ¹³C NMR (D₂O) δ 61.2, 61.4, 66.3, 66.7, 66.9, 68.8, 71.1 (d, $J = 2.6$ Hz), 73.9, 76.3 (dd, $J = 22.9, 26.6$ Hz), 76.9 (t, $J = 22.9$ Hz), 77.9, 79.3, 121.6 (dd, $J = 251.1, 253.9$ Hz); ESIHRMS calcd for C₁₃H₂₂O₁₀F₂Na [M+Na]⁺: 399.1073. Found: 399.1070.

4.15. Molecular modeling

Potential energy surfaces and population maps were calculated using the MM3* force field,²³ as implemented in MACROMODEL 7.1.³² Torsion angle Φ_{Man} is defined as H1Man-C1Man-CF2-C1Gal and Φ_{Gal} as H1Gal-C1Gal-CF2-C1Man. In a first step, a rigid $\Phi_{\text{Man}}/\Phi_{\text{Gal}}$ map was calculated by using a grid step of 18° at each torsion coordinate.^{33,34} The corresponding 400 conformers were optimized by fixing $\Phi_{\text{Man}}/\Phi_{\text{Gal}}$ at each corresponding value to generate the relaxed energy map. The probability distribution was calculated from the energy values according to a Boltzmann function at 300 K. In all the molecular mechanics and dynamics calculations, the GB/SA solvation model for water was used.

The molecular dynamics simulations were also performed using the MM3* force field within MACROMODEL 7.1. For molecular dynamics simulations, several geometries, corresponding to the different low energy minima, were used as input. A temperature simulation of 300 K was employed with a time step of 1.5 fs and an equilibration time of 100 ps. The total simulation times for each compound was 3 ns.

4.16. NMR spectroscopy

¹H NMR (500 MHz) spectra were recorded at 30 °C in D₂O on a Bruker AVANCE 500 spectrometer. Concentrations of ca. 5 mM of **5** were used. Chemical shifts are reported in ppm, using external TMS (0 ppm) as a reference. The 2D-TOCSY experiment (70 ms mixing time) was performed using a data matrix of 256 × 2K to digitize a spectral width of 3000 Hz. Four scans were used per increment with a relaxation delay of 2s. 2D-NOESY (600, 800, and 1000 ms) and 2D-T-ROESY experiments (300, 400, and 500 ms) used the standard sequences. 1D-Selective NOE spectra were acquired using the double echo sequence proposed by Shaka and co-workers at 250, 350, 450, and 550 ms of mixing time.³⁵ Distances were estimated from NOESY/ROESY experimental data as follows: NOE intensities were normalized with respect to the diagonal peak at zero mixing time. Selective T₁ measurements were performed on the anomeric and several other protons to obtain the above-mentioned values. Experimental NOE's were fitted to a double exponential function, $f(t) = p_0(e^{-p_1 t})(1 - e^{-p_2 t})$ with p_0 , p_1 , and p_2 being adjustable parameters.¹² The initial slope was determined from the first derivative at time $t = 0$, $f'(0) = p_0 p_2$. From the initial slopes, inter-proton distances were obtained by employing the isolated spin pair approximation.

All the theoretical NOE calculations were automatically performed by a home-made programme, which is available from the authors upon request.^{33,34}

Acknowledgments

This investigation was supported by Grant R01 GM57865 from the National Institutes of Health (NIH). ‘Research Centers in Minority Institutions’ award RR-03037 from the National Center for Research Resources of the NIH, which supports the infrastructure and instrumentation of the Chemistry Department at Hunter College, is also acknowledged. The group at Madrid thanks the Ministry of Science of Education of Spain (Grant CTQ2006-C02-01) for funding.

Supplementary data

Supplementary data associated with this article can be found, in the online version, at doi:10.1016/j.carres.2007.06.012.

References

- For C-glycoside reviews: (a) Postema, M. H. D. *C-Glycoside Synthesis*; CRC Press: Boca Raton, FL, 1995; (b) Levy, D. E.; Tang, C. *The Synthesis of C-Glycosides*; Pergamon: Oxford, 1995; (c) Beau, J.-M.; Gallagher, T. *Top. Curr. Chem.* **1997**, *187*, 1–54; (d) Togo, H.; He, W.; Waki, Y.; Yokoyama, M. *Synlett* **1998**, 700–717; (e) Du, Y.; Linhardt, R. J.; Vlahov, J. R. *Tetrahedron* **1998**, *54*, 9913–9959; (f) Postema, M. H. D.; Piper, J. L.; Betts, R. L. *Synthesis* **2005**, 1345–1358; (g) Yuan, X.; Linhardt, R. J. *Curr. Top. Med. Chem.* **2005**, *5*, 1393–1430; (h) Levy, D. E. In *The Organic Chemistry of Sugars*; Levy, D. E., Fügedi, P., Eds.; CRC Press/Taylor & Francis: Boca Raton, 2005; pp 269–348.
- For examples of relative activity of O-glycosides and their exact C-glycoside analogues: (a) Acton, E. M.; Ryan, K. J.; Tracy, M.; Arora, S. K. *Tetrahedron Lett.* **1986**, *27*, 4245–4248; (b) Wei, A.; Boy, K. M.; Kishi, Y. *J. Am. Chem. Soc.* **1995**, *117*, 9432–9436; (c) Uchiyama, T.; Vassilev, V. P.; Kajimoto, T.; Wong, W.; Huang, H.; Lin, C.-C.; Wong, C.-H. *J. Am. Chem. Soc.* **1995**, *117*, 5395–5396; (d) Xin, Y.-C.; Zhang, Y.-M.; Mallet, J.-M.; Glaudemans, C. P. J.; Sinaÿ, P. *Eur. J. Org. Chem.* **1999**, 471–476; (e) Link, J. T.; Sorensen, B. K. *Tetrahedron Lett.* **2000**, *41*, 9213–9217; (f) Mikkelsen, L. M.; Hernáiz, M. J.; Martín-Pastor, M.; Skrydstrup, T.; Jiménez-Barbero, J. *J. Am. Chem. Soc.* **2002**, *124*, 14940–14951; (g) Yang, G.; Schmieg, J.; Tsuji, M.; Franck, R. W. *Angew. Chem., Int. Ed.* **2004**, *43*, 3818–3822.
- Jiménez-Barbero, J.; Espinosa, J. F.; Asensio, J. L.; Cañada, F. J.; Poveda, A. *Adv. Carbohydr. Chem. Biochem.* **2001**, *56*, 235–284.
- For an example where O- and C-glycosides bind in different conformations with respect to the intersaccharide torsions: Espinosa, J. F.; Montero, E.; Vian, A.; García, J. L.; Dietrich, H.; Schmidt, R. R.; Martín-Lomas, M.; Imberty, A.; Cañada, F. J.; Jiménez-Barbero, J. *J. Am. Chem. Soc.* **1998**, *120*, 1309–1318.
- (a) Gabius, H.-J. *Pharm. Res.* **1998**, *15*, 23–30; (b) Dam, T. K.; Brewer, C. F. *Chem. Rev.* **2002**, *102*, 387–429.
- Tozer, M. J.; Herpin, T. F. *Tetrahedron* **1996**, *52*, 8619–8683.
- The preferred *gauche* conformation in 2-fluoroethyl residues attached to electronegative substituents is well documented. For recent examples: (a) Briggs, C. R. S.; O’Hagan, D.; Howard, J. A. K.; Yufit, D. S. *J. Fluorine Chem.* **2003**, *119*, 9–13; (b) Briggs, C. R. S.; O’Hagan, D.; Rzepa, H. S.; Slawin, A. M. Z. *J. Fluorine Chem.* **2004**, *125*, 19–25.
- Meier, C.; Knispel, T.; Marquez, V. E.; Siddiqui, M. A.; De Clercq, E.; Balzarini, J. *J. Med. Chem.* **1999**, *42*, 1615–1624.
- Burkholder, C. R.; Dolbier, W. R., Jr.; Médebielle, M. *J. Fluorine Chem.* **2001**, *109*, 39–48.
- (a) Blackburn, G. M.; Kent, D. E.; Kolkman, F. J. *Chem. Soc., Perkin Trans. 1* **1984**, 1119–1125; (b) Thatcher, G. R. J.; Campbell, A. S. *J. Org. Chem.* **1993**, *58*, 2272–2281; (c) Nieschalk, J.; O’Hagan, D. *J. Chem. Soc., Chem. Commun.* **1995**, 719–720.
- For examples of difluoromethylene-linked C-furanosides: (a) Herpin, T. F.; Motherwell, W. B.; Tozer, M. J. *Tetrahedron: Asymmetry* **1994**, *5*, 2269–2282; (b) Herpin, T. F.; Motherwell, W. B.; Weibel, J.-M. *J. Chem. Soc., Chem. Commun.* **1997**, 923–924.
- (a) Asensio, J. L.; Cañada, F. J.; Cheng, X.; Khan, N.; Mootoo, D. R.; Jiménez-Barbero, J. *Chem. Eur. J.* **2000**, *6*, 1035–1041; (b) García-Aparicio, V.; Fernández-Alonso, M.; Angulo, J.; Asensio, J. L.; Cañada, F. J.; Jiménez-Barbero, J.; Mootoo, D. R.; Cheng, X. *Tetrahedron: Asymmetry* **2005**, *16*, 519–527.
- Pérez-Castells, J.; Hernández-Gay, J. J.; Denton, R. W.; Tony, K. A.; Mootoo, D. R.; Jiménez-Barbero, J. *J. Org. Biomol. Chem.* **2007**, *5*, 1087–1092.
- (a) Hiruma, K.; Kajimoto, T.; Weitz-Schmidt, G.; Ollmann, I.; Wong, C.-H. *J. Am. Chem. Soc.* **1996**, *118*, 9265–9270; (b) Hiruma, K.; Kanie, O.; Wong, C.-H. *Tetrahedron* **1998**, *54*, 15781–15792; (c) Shibata, K.; Hiruma, K.; Kanie, O.; Wong, C.-H. *J. Org. Chem.* **2000**, *65*, 2393–2398.
- For a preliminary account on the synthesis of **5** and related fluorinated β -C-galactosides: Tony, K. A.; Denton, R. W.; Dilhas, A.; Jiménez-Barbero, J.; Mootoo, D. R. *Org. Lett.* **2007**, *9*, 1441–1444.
- (a) Khan, N.; Cheng, X.; Mootoo, D. R. *J. Am. Chem. Soc.* **1999**, *121*, 4918–4919; (b) Cheng, X.; Khan, N.; Mootoo, D. R. *J. Org. Chem.* **2000**, *65*, 2544–2547; (c) Denton, R. W.; Cheng, X.; Tony, K. A.; Dilhas, A.; Hernández, J. J.; Canales, A.; Jiménez-Barbero, J.; Mootoo, D. R. *Eur. J. Org. Chem.* **2007**, 645–654.
- (a) Middleton, W. J.; Bingham, E. M. *J. Org. Chem.* **1980**, *45*, 2883–2887; (b) Hägele, G.; Haas, A. *J. Fluorine Chem.* **1996**, *76*, 15–19; (c) Dubowchik, G. M.; Padilla, L.; Edinger, K.; Firestone, R. A. *J. Org. Chem.* **1996**, *61*, 4676–4684.
- (a) Matsumura, Y.; Asai, T.; Shimada, T.; Nakayama, T.; Urushihara, M.; Morizawa, Y.; Yasuda, A.; Yamamoto, T.; Fujitani, B.; Hosoki, K. *Chem. Pharm. Bull.* **1995**, *43*, 353–355; (b) Chang, C. S.; Negishi, M.; Nakano, T.; Morizawa, Y.; Matsumura, Y.; Ichikawa, A. *Prostaglandins* **1997**, *53*, 83–90.
- For the same reaction on related aldehydes: (a) Marcotte, S.; D’Hooge, F.; Ramadas, S.; Feasson, C.; Pannecoucke, X.; Quirion, J.-C. *Tetrahedron Lett.* **2001**, *42*, 5879–5882; (b) Li, Y.; Drew, M. G. B.; Welchman, E. V.; Shirastava, R. K.; Jiang, S.; Valentine, R.; Singh, G. *Tetrahedron* **2004**, *60*, 6523–6531; (c) Karce, N. P.; Pierry, C.; Poulain, F.; Oulyadi, H.; Leclerc, E.; Pannecoucke, X.; Quirion, J.-C. *Synlett* **2007**, 123–126.

20. For aldehyde **11**: Skaanderup, P. R.; Hyltoft, L.; Madsen, R. *Monatsh. Chem.* **2002**, *133*, 467–472.
21. (a) Inanaga, J.; Hirata, K.; Saeki, H.; Katsuki, T.; Yamaguchi, M. *Bull. Chem. Soc. Jpn.* **1979**, *52*, 1989–1993; (b) White, J. D.; Blakemore, P. R.; Browder, C. C.; Hong, J.; Lincoln, C. M.; Nagornyy, P. A.; Robarge, L. A.; Wardrop, D. J. *J. Am. Chem. Soc.* **2001**, *123*, 8593–8595.
22. (a) Takai, K.; Kakiuchi, T.; Kataoka, Y.; Utimoto, K. *J. Org. Chem.* **1994**, *59*, 2668–2670; (b) Postema, M. H. D.; Calimente, D.; Liu, L.; Behrmann, T. L. *J. Org. Chem.* **2000**, *65*, 6061–6068.
23. (a) Pearlman, D. A.; Case, D. A.; Caldwell, J. W.; Ross, W. S.; Cheatham, T. E.; DeBolt, S.; Ferguson, D.; Siebal, G.; Kollmann, P. A. *Comput. Phys. Commun.* **1995**, *91*, 1–41; (b) Allinger, N. L.; Yuh, Y. H.; Lii, J. H. *J. Am. Chem. Soc.* **1989**, *111*, 8551–8566.
24. Asensio, J. L.; Espinosa, J. F.; Dietrich, H.; Cañada, F. J.; Schmidt, R. R.; Martín-Lomas, M.; André, S.; Gabius, H.-J.; Jiménez-Barbero, J. *J. Am. Chem. Soc.* **1999**, *121*, 8995–9000.
25. (a) Poveda, A.; Asensio, J. L.; Polat, T.; Bazin, H.; Linhardt, R. J.; Jiménez-Barbero, J. *Eur. J. Org. Chem.* **2000**, 1805–1813; (b) Montero, E.; García-Herrero, A.; Asensio, J. L.; Hirai, K.; Ogawa, S.; Santoyo-González, F.; Cañada, F. J.; Jiménez-Barbero, J. *Eur. J. Org. Chem.* **2000**, 1945–1952, and references cited therein.
26. For a discussion on the application of molecular mechanics force fields to sugar molecules, see: Perez, S.; Imberty, A.; Engelsen, S.; Gruza, J.; Mazeau, K.; Jimenez-Barbero, J.; Poveda, A.; Espinosa, J. F.; van Eyck, B. P.; Johnson, G. *Carbohydr. Res.* **1998**, *314*, 141–155.
27. Neuhaus, D.; Williamson, M. P. *The Nuclear Overhauser Effect in Structural and Conformational Analysis*; VCH: New York, 1989.
28. Bock, K.; Duus, J. O. *J. Carbohydr. Chem.* **1994**, *13*, 513–543.
29. Haasnoot, C. A. G.; de Leeuw, F. A. A. M.; Altona, C. *Tetrahedron* **1980**, *36*, 2783–2794.
30. (a) Thibaudeau, C.; Plavec, J.; Chattopadhyaya, J. *J. Org. Chem.* **1998**, *67*, 4967–4984; (b) Karplus, M. *J. Chem. Phys.* **1959**, *30*, 11–15.
31. (a) Velter, I.; Nicotra, F.; Laferla, B.; Bernardi, A.; Marcou, G.; Motto, I.; Mari, S.; Cañada, F. J.; Jimenez-Barbero, J. *Eur. J. Org. Chem.* **2006**, 2925–2933; (b) Mari, S.; Sánchez-Medina, I.; Jimenez-Barbero, J.; Bernardi, A. *Carbohydr. Res.*, this issue.
32. Mohamadi, F.; Richards, N. G. J.; Guida, W. C.; Liskamp, R.; Caufield, C.; Chang, G.; Hendrickson, T.; Still, W. C. *J. Comput. Chem.* **1990**, *11*, 440–467.
33. Espinosa, J. F.; Martín-Pastor, M.; Asensio, J. L.; Dietrich, H.; Martín-Lomas, M.; Schmidt, R. R.; Jiménez-Barbero, J. *Tetrahedron Lett.* **1995**, *36*, 6329–6332.
34. Asensio, J. L.; Martín-Pastor, M.; Jiménez-Barbero, J. *Int. J. Biol. Macromol.* **1995**, *17*, 137–148.
35. Stott, K.; Stonehouse, J.; Keeler, J.; Hwang, T. L.; Shaka, A. J. *J. Am. Chem. Soc.* **1995**, *117*, 4199–4200.